

3D Numerical Study of Time Dependent Bed Changes in the Flushing Channels for Free Flow Sediment Flushing in Reservoirs

Taymaz ESMAEILI⁽¹⁾, Tetsuya SUMI, Yasuhiro TAKEMON and Sameh A. KANTOUSH⁽²⁾

(1) Ph.D. student, Dept. Of Urban Management, Graduate School of Engineering, Kyoto University

(2) Assoc. Professor, Dept. Of Civil Engineering, German University Cairo (GUC)

Synopsis

Dams are extensively used for different purposes (i.e. irrigation, water supply, flood control and hydro-electric power supply) and flushing is one of the proposed methods for preserving the storage capacity of dam reservoirs. In the free-flow sediment flushing, the water level is drawdown during a flood and subsequently the increase in the flow velocity results in sediment erosion in dam reservoir. The efficiency of the free-flow sediment flushing depends on various parameters such as hydraulic condition, sediment properties and reservoir geometry. Owing to this fact that advanced numerical models could simulate many aspects of the hydraulic characteristic of flow and sediment erosion-deposition field, application of these models could provide the initial assessment of the different impacts of upcoming free-flow sediment flushing. In the present study a fully 3D numerical model, SSIIM, used for assessing the temporal bed changes during the free-flow sediment flushing in various shallow reservoir geometries. The outcomes of the numerical simulations reveal the capability of the 3D numerical model to simulate the different stages of channel formation in shallow reservoirs and also modeling the flow field when the bed topography is in the equilibrium condition.

Keywords: Reservoir sedimentation, 3D numerical simulation, free-flow sediment flushing

1. Introduction

One of the most important side effects of dam construction over the streams is disturbing the natural sediment transport trend from upstream to the downstream area. When the stream flow enters a dam reservoir, the flow velocity decreases and subsequently in such a condition, all bed load and all or a portion of the suspended load deposits in the dam reservoir. Also, the fine sediments are transported deeper into the reservoir by the flow. Deposition of sediment reduces the storage capacity of the dam reservoir during the operational period

of dam. The annual rate of reservoir storage capacity loss to sedimentation in the world is 0.5-1% and it varies dramatically from river basin to river basin due to the different forest cover and geological conditions (White 2001). A decreased storage volume reduces the amount of water for flood control purpose, electricity production and water supply. This loss of storage volume represents a huge economic loss and the reduction of flood control benefits (Morris & Fan, 1998). Moreover, in some areas with sedimentation rates above the average (e.g. China 2.3% or the Middle East 1.5%) the lifetime of the dam would be

reduced drastically. Furthermore, the sediment yields of the Japanese rivers are high in comparison with other countries due to the topographical, geological and hydrological conditions (Sumi, 2006).

In order to control the reservoir sedimentation, different approaches such as bypassing, dredging, flushing, sluicing and upstream sediment trapping have been developed. Although the combination of these sediment control measures usually adopted to gain the maximum effect, the flushing and sluicing method plays an important role in the sediment removal and reduction, especially the flushing approach, as it is an efficient hydraulic sediment removal technique to restore the reservoir storage capacity (Liu et al. 2004). Free-flow sediment flushing through dam reservoirs is one of the typical techniques in Japan because of sufficient rain fall, economical issues, independency from other facilities and potential for high efficiency. During the free-flow sediment flushing, the bottom outlets of the dam are opened and the water level in dam reservoir is drawdown in a short time. This process will increase the flow velocity and the bed shear stress, results in forming a channel through deposited sediment in reservoir and flushing the fine and coarse sediment. In some cases, the free-flow sediment flushing is performed during a flood event, with respect to a speculated standard, to facilitate the sediment discharge out and also preventing the negative environmental effects in the downstream. The coordinated free-flow sediment flushing in DASHIDAIRA & UNAZUKI dam reservoir in Kurobe River, located in Toyama prefecture, is a pioneer example as shown schematically in Fig. 1.

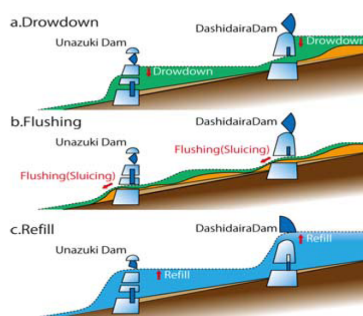


Fig. 1 Outline of coordinated sediment flushing (Minami et al. 2012)

Many reservoirs are not flushed because an accurate prediction of the success of an upcoming reservoir flushing is time and cost-intensive (Haun & Olsen 2012). Loss of the stored water besides the lack of knowledge about the amount of the flushed out sediment and location of the erosion-deposition area in the reservoir will be the negative factors for choosing the free-flow sediment flushing. Following that, the environmental effects downstream of the reservoir caused by the flushing are difficult to estimate because of the complexity of free-flow sediment flushing process. So, it is important to have an initial assessment of the efficiency of upcoming free-flow sediment flushing.

The common way is physical model study that is time consuming, usually not cost effective for complex natural geometries and also takes a long time. The other issue relates to the physical modeling is scale effects which will be further magnified if the fine sediments should be used.

The RESCON model developed by the World Bank in 1999, including the theoretical formulas suggested by Atkinson (1996), to predict the economical feasibility of different approaches for removing the accumulated sediment through dam reservoirs. More specifically, this model is a computer model of RESCON approach developed as a demonstration tool (Palmier et al. 2003). However, results are likely to vary noticeably owing to the reservoir and sediment characteristics. Subsequently this approach is only recommended for use in early design stages as a preliminary study. However, an accurate assumption of the deposition pattern is not feasible with these theoretical formulas (White & Bettes 1984).

Numerical models were developed as an alternative over the last decades to avoid scaling problems and because of an expected time and cost reduction (Chandler et al. 2003). Niu (1987) & Ju (1990) used one-dimensional diffusion model for simulating the volume of flushed out sediment and bed deformation change during the flushing process. One dimensional numerical model usually uses some assumptions and simplifications that could not represent the real nature of complex interacting flow-sediment field during the flushing process. Kitamura (1995) and Zigler & Nisbet (1996) use the

one-dimensional numerical model with a forming flushing channel as limiting factor. More advanced two-dimensional numerical models were used by Olsen (1999) & Badura et al. (2008) for simulating the flushing in a physical model scale and prototype scale respectively.

Three-dimensional numerical models are still under development for application in this field. Atkinson (1996), Khosronejad (2008) and Haun & Olsen (2012) used three-dimensional models for simulating the flushing process in the physical model scale. Application of three-dimensional numerical models for simulating the complex structure of interacting flow and sediment field would be useful for understanding the different stages of flushing process and utilize the outcomes for application in the prototype scale.

In the Present study, Three-dimensional numerical program SSIIM (Simulation of Sediment Movements In Water Intakes With Multiblock Option) was used for simulating the flow field and bed changes when the free-flow sediment flushing is conducted in shallow reservoirs with different geometries.

2. Numerical model SSIIM

2.1 Three dimensional flow model

The SSIIM program solves the Navier-Stokes equations with the k-ε model on a three dimensional general non-orthogonal coordinates. These equations are discretized with a control volume approach. The SIMPLE or SIMPLEC methods can be used for solving the pressure-poisson equation. An implicit solver is used, producing the velocity field in the computational domain. The velocities are used when solving the convection-diffusion equations for different sediment sizes (Olsen 2011).

The Navier-Stokes equations for non-compressible and constant density flow can be modeled as:

$$\frac{\partial u_i}{\partial x_i} = 0 \quad (1)$$

$$\frac{\partial u_i}{\partial t} + u_j \frac{\partial u_i}{\partial x_j} = \frac{1}{\rho} \frac{\partial}{\partial x_j} \left(-P \delta_{ij} - \rho \overline{u_i' u_j'} \right) \quad (2)$$

where the first term on the left side of the Equation (2) is the transient term. The next term is the convective term. The first term on the right-hand side is the pressure term and the second term on the right side of the equation is the Reynolds stress term. In order to evaluate this term, a turbulence model is required. SSIIM program can use different turbulence models, such as the standard k-ε model or the k-ω model by Wilcox (2000). However, the default turbulence model is the standard k-ε model.

The free surface is modeled as a fixed-lid, with zero gradients for all variables. The locations of the fixed lid and its movement are as a function of time, which can be computed by different algorithms. The 1D backwater computation is the default algorithm and it is invoked automatically. Pressure and Bernoulli algorithm can be used for both steady and unsteady computations. The algorithm is based on the computed pressure field. It uses the Bernoulli equation along the water surface to compute the water surface location based on one fixed point that does not move. The algorithm is fairly stable, so that it can also be used in connection with computation of sediment transport and bed changes (Olsen 2011).

For the wall boundary treatment, it is assumed that the velocity profile follows a certain empirical function called a wall law. It is a semi-analytical function to model the turbulence near the wall in the boundary layer and consequently the CFD model will not need to resolve the turbulence of flow in boundary layer. As a result, it would not necessary too many grid points near the wall:

$$\frac{U}{u_x} = \frac{1}{\kappa} \ln \left(\frac{30y}{k_s} \right) \quad (3)$$

where the shear velocity is denoted u_x , κ is a constant equal to 0.4, y is the distance to the wall and k_s is the roughness equivalent to a diameter of particles on the bed.

2.2 Morphological model

The sediment transport process in rivers is described by the following equation, Exner's equation, which is the sediment continuity equation

integrated over the water depth:

$$(1-\lambda)\frac{\partial z_b}{\partial t} + \frac{\partial q_{rx}}{\partial x} + \frac{\partial q_{ry}}{\partial y} = 0 \quad (4)$$

where z_b is the bed elevation, λ is the porosity of bed material, and q_{rx} and q_{ry} are components of total-load sediment transport in x- and y-directions, respectively.

In this 3D CFD program, the suspended load can be calculated with the convection-diffusion equation for the sediment concentration, which is expressed as follows:

$$\frac{\partial c}{\partial t} + u_j \frac{\partial c}{\partial x_j} + w \frac{\partial c}{\partial z} = \frac{\partial}{\partial x_j} (\Gamma_T \frac{\partial c}{\partial x_j}) \quad (5)$$

where w is the fall velocity of sediment particles and Γ_T is the diffusion coefficient and can be expressed in the following way:

$$\Gamma_T = \frac{v_T}{Sc} \quad (6)$$

where Sc is the Schmidt number representing the ratio of diffusion coefficient to eddy viscosity coefficient v_T and set to 1.0 as default.

For calculating the suspended load in Equation (4), Equation (5) is solved incorporated with the formula by van Rijn (1987) for computing the equilibrium sediment concentration close to the bed as the bed boundary. In order to solve Equation (4) and Equation (5), conditions of z and C should be given at inflow and outflow boundaries. For the inlet boundary, due to the clear water scour conditions, $z=C=0$ can be given and for the outlet boundary, far away from the pier, $\frac{\partial C}{\partial x} = \frac{\partial z}{\partial x} = 0$ can be given due to the uniform flow.

The concentration formula has the following expression:

$$C_{bed} = 0.015 \frac{d^{0.3}}{a} \frac{\left[\frac{\tau - \tau_c}{\tau_c} \right]^{1.5}}{\left[\frac{(\rho_s - \rho_w)g}{\rho_w v^2} \right]^{0.1}} \quad (7)$$

where, C_{bed} is the sediment concentration, d is

the sediment particle diameter, a is a reference level set equal to the roughness height, τ is the bed shear stress, τ_c is the critical bed shear stress for movement of sediment particles according to Shield's curve, ρ_w and ρ_s are the density of water and sediment, v is the viscosity of the water and g is the acceleration of gravity.

Once Equation (5) is solved, the suspended load can be calculated as follows:

$$q_{s,i} = \int_a^{z_f} u_i c dz \quad (8)$$

where $q_{s,i}$ ($i=1,2$) are components of suspended-load sediment transport in x-and y-directions, respectively.

For calculating the bed load in Equation (4), the following relation proposed by van Rijn's formula (1987) is used:

$$\frac{q_b}{D_{50}^{1.5} \sqrt{\frac{(\rho_s - \rho_w)g}{\rho_w}}} = 0.053 \frac{\left[\frac{\tau - \tau_c}{\tau_c} \right]^{1.5}}{D_{50}^{0.3} \left[\left(\frac{(\rho_s - \rho_w)g}{\rho_w v^2} \right) \right]^{0.1}} \quad (9)$$

where D_{50} is the mean size of sediment. Then, the components of bed-load sediment transport in x- and y-directions can be calculated as follows:

$$q_{bx} = q_b \cos(\alpha_b); q_{by} = q_b \sin(\alpha_b) \quad (10)$$

where α_b is the direction of bed-load sediment transportation.

3. Experimental conditions

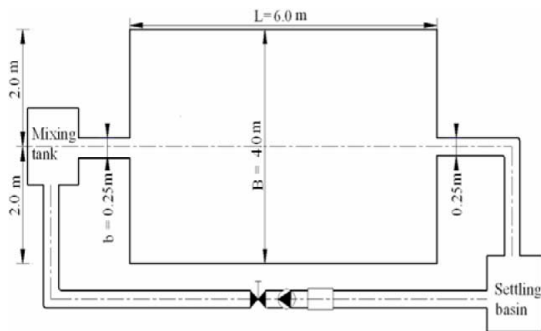
3.1 Experimental set-up

In this paper experimental data provided by Kantoush & Schleiss (2009) were employed. All experimental tests were conducted in a rectangular shallow basin and width of the inlet and outlet was 0.25 m for all cases.

Adjacent to the reservoir, a mixing tank was used to prepare the water-sediment mixture. The water-sediment mixture was supplied by gravity into the water-filled rectangular basin. The

sediments were added to the mixing tank during the test. To model the suspended sediment currents in the laboratory, non-uniform crushed walnut shells with the median grain size (d_{50}) of 50 μm and density of 1500 kg/m^3 was used in all experiments. This is a non-cohesive, light weight and homogeneous grain material (Kantoush & Schleiss 2009). The Ultrasonic Velocity Profiler (UVP) as well as Large Scale Particle Image Velocimetry technique (LSPIV) used for measuring the surface velocity field. The evolution of the bed level was measured with a miniature echo sounder. The hydraulic and sediment condition were set to fulfill the requirements for subcritical and fully developed turbulent flow condition. The water discharge and water level was equal to 0.007 m^3/s and 0.2 m respectively and they were kept constant for the experimental runs. Fig. 2 illustrates the experimental set-up of the reference rectangular basin.

(a)



(b)



Fig. 2 (a) plan view and (b) view looking over the downstream of experimental set-up (Kantoush & Schleiss 2009).

3.2 Test procedure

Kantoush & Schleiss (2009) configured the tests

in three phases. In the first phase the shallow basins filled with clear water and after reaching to the stable state, in the second phase, the mixture of water-sediment drained by the gravity into the water-filled reservoir. In this stage the flow velocity as well as the bed morphology measurements conducted in every 90 minutes interval for a total period of 4.5 hours. The pump was turned off after each time step to record the bed morphology.

In the third phase two types of free-flow flushing (with and without drawdown) performed. The final bed topography from the second phase was used as the initial bed for two types of flushing. Moreover, the clear water introduced into the basin to evaluate the effect of sediment flushing on the bed deformation and the distribution of the horizontal flow velocity pattern. In the case of free-flow flushing with drawdown the water level decreases to half of the normal water depth (0.1 m) whereas it was kept constant in the case without drawdown. The duration of runs was 48 hours but there was no noticeable change in the bed morphology and flow character after about 24 hours.

4. Numerical simulation

4.1 Domain description

In the present study, shallow reservoirs with different geometries were considered to represent the capability of three-dimensional numerical model for assessing the flow velocity distribution and also bed topography changes during the free-flow flushing. Fig. 3 demonstrates the four different types of reservoir geometries (T1, T8, T11 and T13) that were used for the numerical study. T8, T11 and T13 used for modeling the surface flow velocity distribution. Free-flow flushing without drawdown was conducted for run T1 while free-flow flushing with drawdown employed for T8 and T13.

Regarding the procedure of the experimental runs described in the preceding section, in numerical simulations, the final bed morphology obtained in the second phase was used as the initial bed topography before free-flow sediment flushing procedure. Moreover, the final bed morphology in the equilibrium condition was utilized for

simulating the three-dimensional flow field.

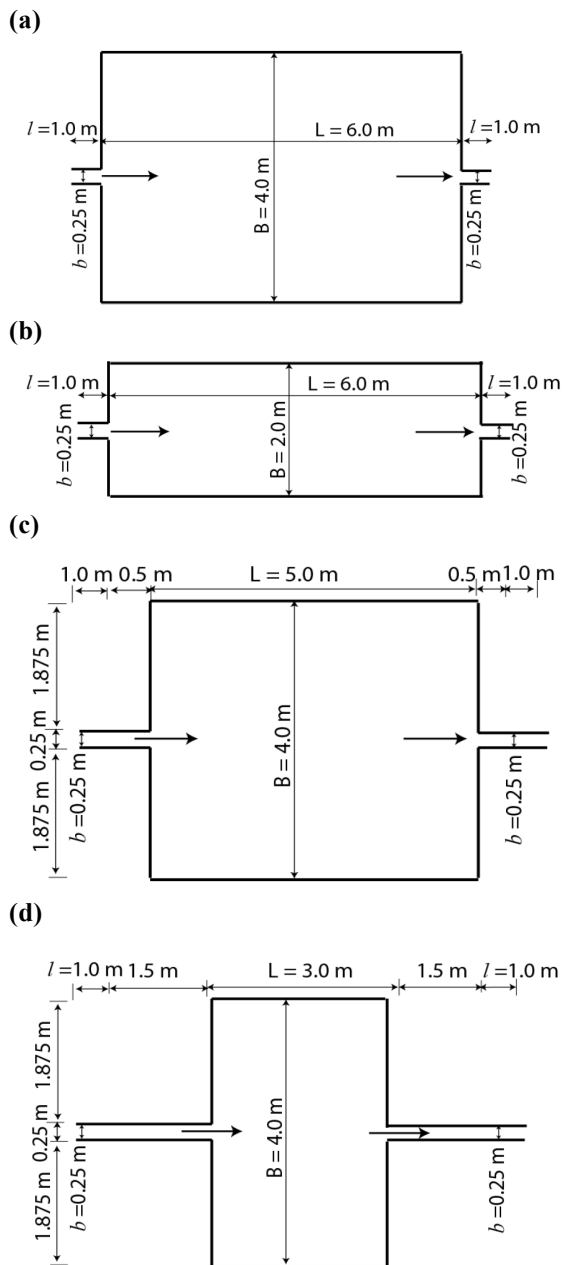


Fig. 3 Geometrical configuration of (a) run T1, (b) run T8, (c) run T11 and (d) run T13.

Making an appropriate grid is a very important process in the preparation of input data for SSIIM program. The size and alignment of the cells will strongly influence the accuracy, the convergence and the computational time (Olsen 2011).

The cell sizes for T1, T8, T11 and T13 in X and Y direction were $5 \text{ cm} \times 2.5 \text{ cm}$, $5 \text{ cm} \times 1.5 \text{ cm}$, $2.5 \text{ cm} \times 1 \text{ cm}$ and $2.5 \text{ cm} \times 1 \text{ cm}$ respectively. Considering the 12 cells for vertical grid

distribution, the total number of cells were 230400, 190320, 960000 and 576000 respectively.

For the inflow boundary condition, the velocity distribution was specified by the numerical model while the gradient of pressure is given zero. At the outflow boundary, the vertical gradient of velocity is zero and the hydrostatic pressure distribution is specified according to the water depth. For the solid boundary, wall laws introduced by Schlichting (1979) were used for the side walls and the bed.

During the simulations it was found that it is important to model the drawdown procedure appropriately for T8, T11 and T13 runs. So, the water level in the reservoir lowered during a short period of time (about 1.5 minutes) to the half and subsequently due to the increased flow velocity and bed shear stress the flushing channel start to form along the reservoir. Because of the hydraulically complex nature of the drawdown and then flushing channel formation, it is necessary to adjust the roughness, time step, discretization method and sediment related parameters to get the satisfying results with respect to the measured experimental data. So, because of the shallow water condition and also different expansion ratio it is necessary to check different set of input parameters. Moreover, some simplification in sediment size distribution was assumed in order to introduce the non-uniform sediments to the model.

4.2 Simulation of flow velocity field

Measuring the surface velocity using LSPIV (Large Scale Particle Image Velocimetry) is usually conducted as a part of monitoring process during the free-flow sediment flushing from dam reservoirs (i.e. Unazuki and Dashidaira reservoirs in Japan). Furthermore, measuring the flow velocity during the flushing process can help us to better understand of the erosion and deposition dynamic during the flushing.

Owing to the importance of the flow velocity measurement after full draw down, the simulated flow velocity field by the numerical model SSIIM compared to that of measured during the experimental runs. So, the final bed morphology after the free-flow sediment flushing with drawdown introduced to the model and the three-dimensional flow field was calculated.

Fig. 4 shows the simulated surface velocity distribution pattern versus the measured one for runs T8, T11 and T13 respectively.

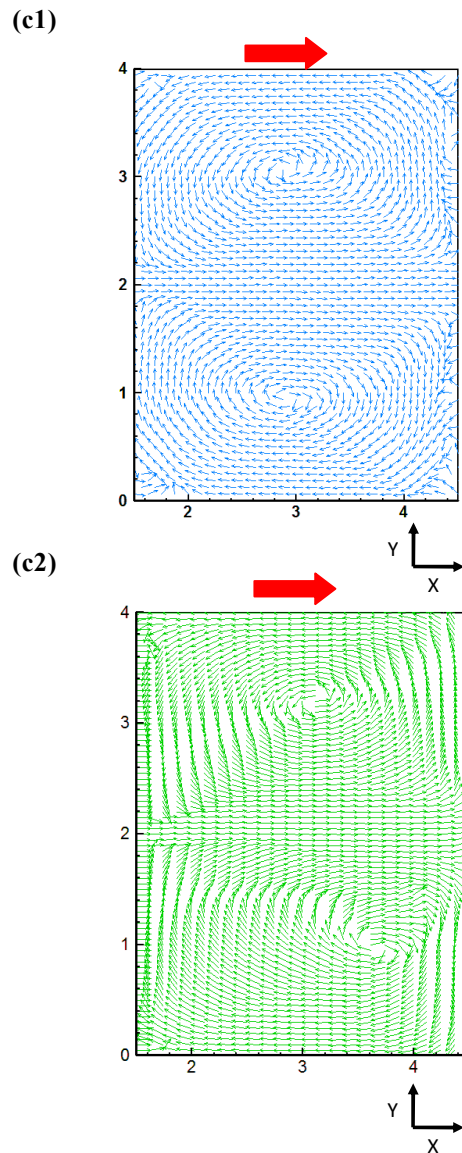
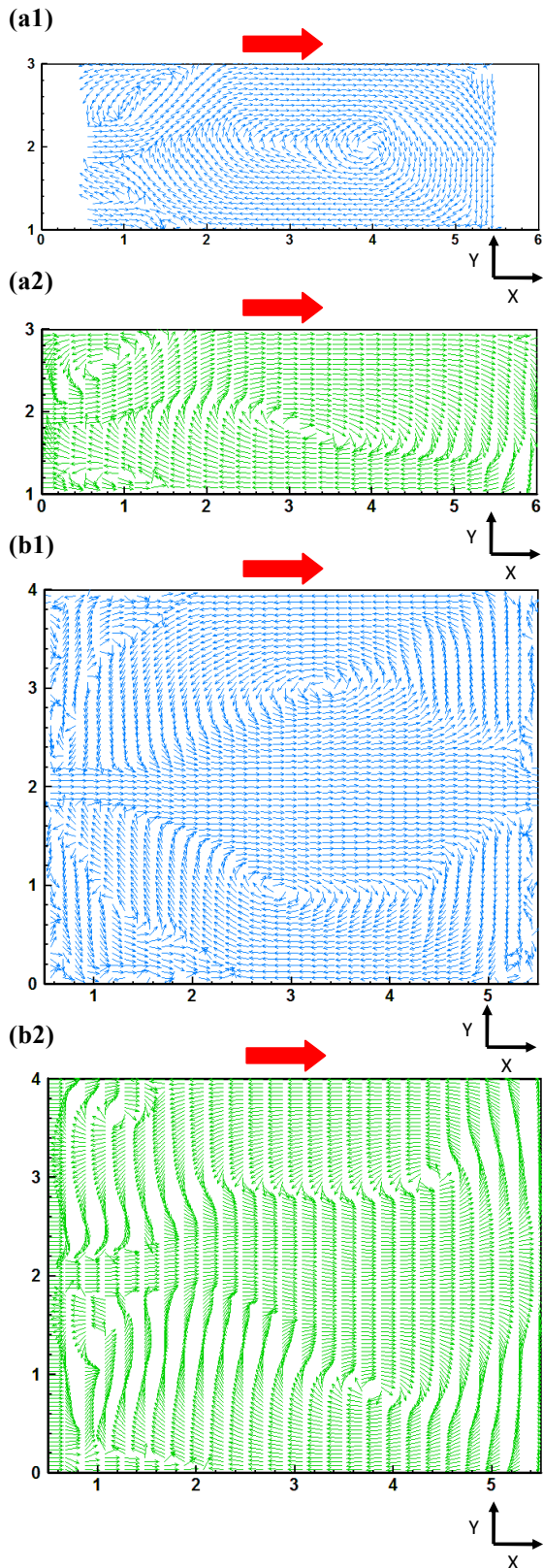


Fig. 4 (a1), (b1) and (c1) measured surface velocity and (a2), (b2) and (c2) simulated surface velocity for run T8, T11 and T13 respectively. The flow direction is from left to right.

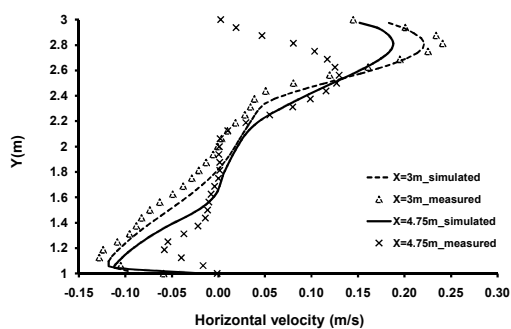
Fig. 5 illustrates the simulated and measured horizontal velocity distribution in transversal direction at the water surface. The measurements were in two positions, namely the middle and downstream half of the channel. The downstream half position was $X=4.75\text{m}$ for T8 and $X=4\text{m}$ for T11 and T13.

As can be clearly observed from the Fig. 4, the model could simulate the surface flow velocity pattern, almost similar to the measured one, with the main aspects such as the flow velocity direction

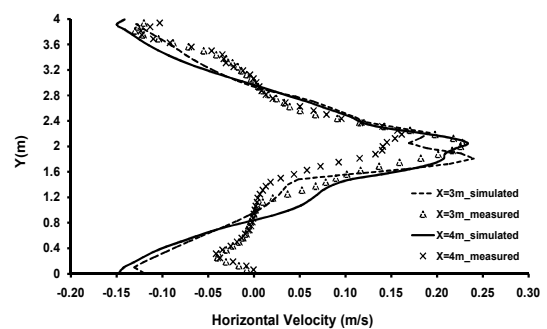
and the position of different eddies and circulation areas. As for the surface velocity of run T8, the simulation shows the asymmetric flow structure similar to the measurements but the recirculation zone beside the right wall is different than obtained by the measurements. Concerning the T11 and T13 run, the symmetric flow pattern with two distinguished circulation zones on the both sides can be observed in the simulation outputs. But, still the circulation domain and consequently the main high flow velocity trajectory field is not completely similar to the measurements. Furthermore, Fig. 5 reveals that although the numerical model quantitatively could simulate the magnitude of the horizontal flow velocity in the water surface, results has better agreement with the measured values in the middle of the channel than the downstream half. It is obvious that the flow field in the downstream half is more complex because of the strong reverse flow formation while a portion of the stream flow discharged out from the outlet gate. The discrepancy between simulated and measured flow velocities beside the walls is higher than other areas. As mentioned before, it is assumed that the velocity profile follows a certain empirical functions whereas reverse flows accompanying with eddies present a complex flow field beside the walls.

However during the simulations it was found that the lateral expansion ratio (reservoir width/inlet width) and aspect ratio (reservoir length/reservoir width) when the total area of the reservoir is same, are important parameters which can strictly affect the stability and also the accuracy of the numerical model results.

(a)



(b)



(c)

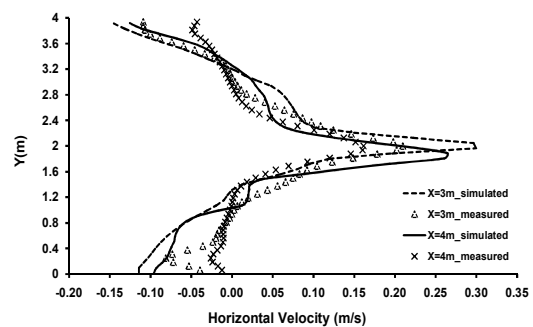


Fig. 5 Horizontal surface velocity in the transversal direction for (a) T8, (b) T11 and (c) T13.

More specifically, the total area of runs T8 and T13 are same but the flow field computation was much more stable in run T8 than run T13.

4.3 Simulation of bed changes and flushing channel formation

Drawdown is the lowering of the water level in a reservoir. Hydraulic flushing involves reservoir drawdown by opening the bottom outlet to generate and accelerate unsteady flow towards the outlet (Morris & Fan, 1998). This process will initiate the progressive and retrogressive erosion pattern in the deposited sediment that leads in to formation of the flushing channels in the reservoir.

Nonetheless, investigation and explanation about formation and also the characteristic of flushing channel in different type of reservoirs is necessary. The characteristic of the flushing channel when the reservoir is fully drawdown can be briefly introduced by the location, width, side and longitudinal slope and shape.

In this paper a free-flow flushing without drawdown for the run T1 and with drawdown for

the run T8 and T13 were conducted by employing the three-dimensional numerical model SSIIM. The simulated final bed morphology was compared to the measured data by Kantoush & Scleiss (2009). Fig. 6 demonstrates the final measured and simulated bed topography contours for T1, T8 and also T13. Because the equilibrium condition was obtained after one day, the simulation period for bed changes was 24 hours. In order to further discussion about the characteristics of flushing channel formation, the cross-section change caused by lateral bank erosion in the middle of the reservoir has been shown for T8 and T13 in Fig. 7. Also, Fig. 7c provides data about degradation along the center line of T13 reservoir.

For the run T1, the final bed topography obtained in phase 2, used as the initial topography. Then, the clear water without sediment injected into the reservoir with the constant hydraulic condition ($Q=7$ l/s and $h=0.2$ m). As shown in Fig. 6a and 6b, if the flushing is performed with the constant water level, sediment will be flushed from a very small area mostly close to the inlet. In such a condition, the free-flow flushing effect would be very local and tongue-shaped crater topography would be visible (Fig. 6a and 6b).

In free-flow flushing with drawdown, the water level lowering will generate high flow velocity that initiates the flushing channel formation. The erosion pattern along with strong jet flow, then, develops the initial flushing channel geometry. In this stage the initial flushing channel deepened and widened. The location of the flushing channel depends on the flow characteristic and reservoir geometry. In the next stage, during a relatively short period, a rapid widening of the flushing channel with an advancing front is visible.

Fig. 6d and 6f reveals that in the simulation results for both T8 and T13 runs, the flushing channel location was in the centerline along the shortest path between the inlet and outlet whereas measured data demonstrate the flushing channel development direction is towards the left side in the run T8. Both the simulation outputs and the experimental measured bed, illustrate the same location for the flushing channel in the run T13. Moreover, the measured final bed topography shows that the channel width increased in the

downstream direction similar to a T shape head. The same trend witnessed in the simulation results (Fig. 6e & 6f). However, the sediment deposition pattern in the simulation seems different, although there are some similarities. So, the various set of input parameters should be employed to have more accurate bed deposition pattern.

The bed topography, geometry of the reservoir and also flow pattern developed by the entrance jet can affect the location, size and shape of the flushing channel. However, the final bed deposition pattern would also able to change the flow pattern. So, deviation of the jet trajectory from the short and straight path from inlet to the outlet likely to result in different characteristic of scoured channel. Regarding the run T8, this can be the reason for different location, size and shape of the flushing channel in the simulation and measurement.

5. Conclusions

In this paper, first, the final measured surface velocity using the LSPIV technique compared with the simulation results utilizing the three-dimensional numerical model SSIIM. In the next step, free flow flushing without drawdown for one case and with drawdown for two cases were performed. The following results obtained from the study:

- 1- The SSIIM model can simulate the complex characteristics of the surface velocity using the equilibrium final bed morphology, almost similar to the measured one. Many aspects such as jet trajectory, recirculation zones, eddies and the flow distribution pattern can be presented quantitatively. In addition, comparing the simulated horizontal surface velocity to the measured one reveals the capability of the numerical model for quantitatively assessing the surface flow velocity.
- 2- Free-flow flushing without drawdown had only a very local effect. Small nosed shape flushing channel emerged close to the inlet and it did not expand and distribute to the downstream direction. Nevertheless, a small cone shaped erosion area appeared beside the outlet in the numerical simulation results.

3- During the free-flow flushing for two geometry type reservoirs (namely wide and narrow), straight flushing channel along the centerline formed in numerical simulations. On the other hand, experimental runs show

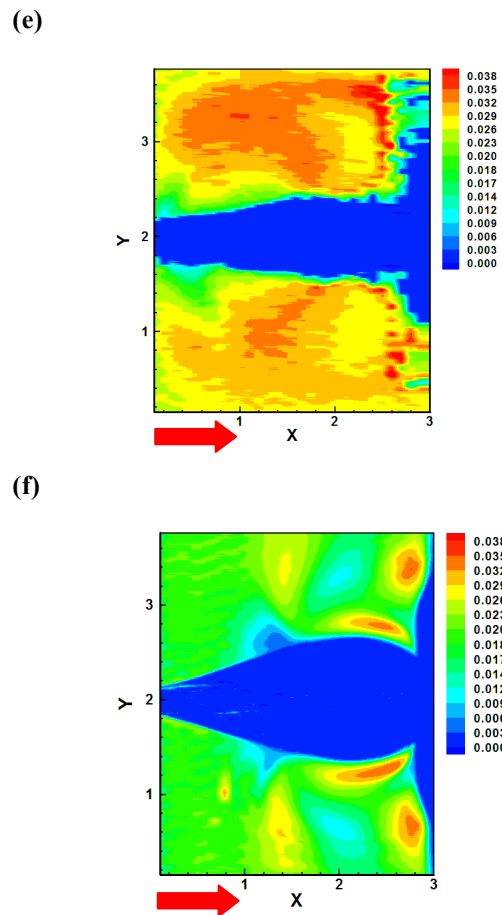
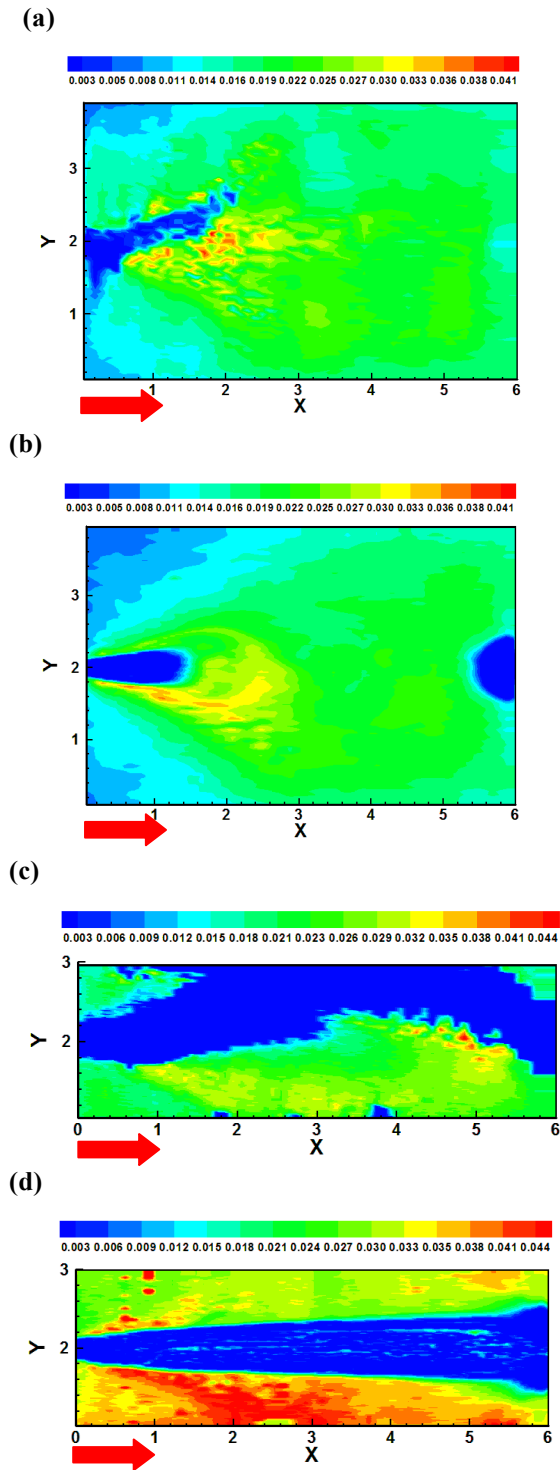


Fig. 6 Contours of measured bed after flushing for (a) T1, (c) T8 and (f) T13 versus simulated bed contours for (b) T1, (d) T8 and (f) T13.

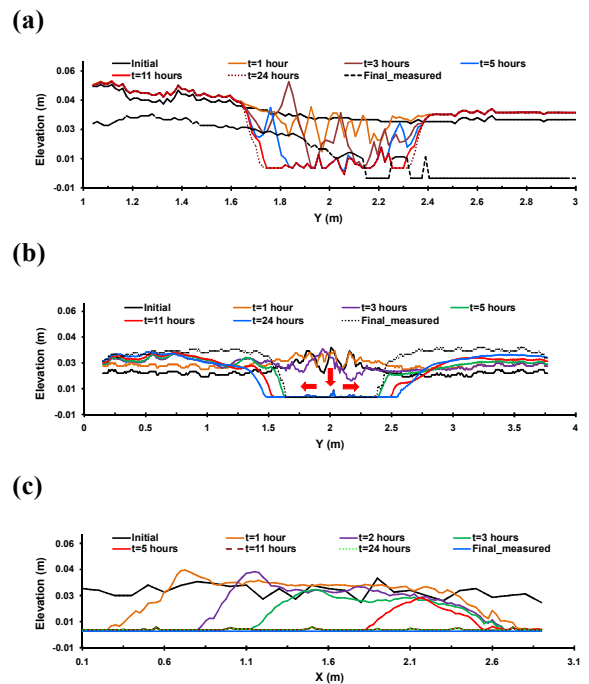


Fig. 7 Lateral development of flushing channel for (a) T8 and (b) T13 during the free-flow flushing

with drawdown; (c) Channel degradation along the centerline of reservoir T13.

the different location of the flushing channel for narrow reservoir. Reservoir geometry, bed topography, flow pattern affect the location, size and shape of the flushing channel and at the same time, the final bed topography has the potential to influence the flow pattern. In addition, the flow pattern is important to boundary condition. Owing to the dynamic interaction between various effective parameters, the exact prediction of the geometrical character of flushing channel is difficult. In addition, a deviation in the entrance flow would have a major effect on flushing channel formation procedure.

4- Although the location, shape and size of the flushing channel are important, it is necessary to have the insight about the upcoming flushing efficiency. Specifically, estimating the volume of the flushed out sediment by numerical model would be useful both from the hydraulic and environmental point of view. The numerical models, especially three-dimensional models with reasonable accuracy, can be a cost-effective and also time-saving alternative for physical experiments. Furthermore, various shapes of reservoirs should be considered in order to evaluate different geometric and hydraulic aspects of flushing channel formation in the future studies.

References

Atkinson, E., (1996): The feasibility of flushing sediment from reservoirs, Tech. report, HR Wallingford, UK.

Badura, H., Knoblauch, H. and Schneider, J. (2008): Pilot project Bodendorf, Work Package 8 " Pilot Actions ". Report of the EU Interreg IIIB Project ALPRESREV, Austria.

Chandler, K., Gill, D., Maher, B., Macnish, S. and Roads, G. (2003): Cooping with maximum probable flood-an alliance project delivery for Wivenhoe Dam, Proceedings of 43rd conference, Hobart, Tasmania.

Haun, S. and Olsen, N. R. B. (2012): Three-dimensional numerical modeling of reservoir flushing on a prototype scale, *Int. J. River Basin Management*, Vol., (10), No. 4, pp. 341-349.

Ju, J., (1990): Computational method of headwater erosion and its application, *Journal of Sediment Research*, Vol. (1), 30-39 (In Chinese).

Kantoush, A. S. and Schleiss, A. J. (2009): Channel formation during flushing of large shallow reservoirs with different geometries, *Environmental Technology*, Vol. (30), No. 8, pp. 855-863.

Khosronejad, A., Rennie, C.D., Salehi Neyshabouri, A.A. and Gholami, I. (2008): Three dimensional numerical modeling of sediment release, *Journal of Hydr. Research*, Vol. (46), No. 2, pp. 209-223.

Kitamura, Y., (1995): Erosion and transport process of cohesive Sediments in dam reservoirs, *Journal of Hydroscience and Hydraulic Engineering*, Vol. (13), No. 1, pp. 47-61.

Liu, J., Minami, S., Otsuki, H., Liu, B. and Ashida, K. (2004): Prediction of concerted sediment flushing, *Journal of Hydr., Eng., ASCE*, Vol. (130), No. 11, pp. 1089-1096.

Minami, S., Noguchi, K., Otsuki, H., Fukuroi, H., Shimahara, N., Mizuta, J. and Takeuchi, M. (2012): Coordinated sediment flushing and effect verification of fine sediment discharge operation in Kurobe River, Proceedings of the International symposium on dams for changing world, ICOLD, Kyoto, Japan.

Morris, G. L., & Fan, J. (1998): *Reservoir Sedimentation Handbook*, New York: McGraw-Hill Inc.

Olsen, N. R. B., (1999): Two-dimensional modeling of flushing process in water reservoirs, *Journal of Hydraulic Research*, Vol. (37), No. 1, pp. 3-16.

Olsen, N. R. B., (2011): A three-dimensional numerical model for simulation of sediment movements in water intakes with multiblock option, www.ntnu.no, Online User's manual.

Palmier, A., Shah, F., Annandale, G.W. and Dinar, A. (2003): *Reservoir Conservation Volume 1: The RESCON approach*, World Bank.

Schlichting, H. (1979): *Boundary-Layer Theory*, New York: Mc-Graw Hill Inc.

Sumi, T., 2006: Reservoir sediment management measure and necessary instrumentation technologies to support them, The 6th Japan-Taiwan Joint Seminar on Natural Hazard Mitigation.

White, W.R. and Bettess, R. (1984): The feasibility of flushing sediment through reservoirs. Challenges in African Hydrology and Water Resources. Proceedings of the Harare Symposium, IAHS press, Wallingford, UK.

White, R., (2001): Evacuation of sediments from reservoirs, Thomas Telford Press.

Wilcox, D.C. (2000): Turbulence modeling for CFD, California: DCW Industries Inc.

Ziegler, C.K. and Nisbet, B.S. (1995): Long term simulation of fine-grained sediment transport in large reservoir, Journal of Hydr., Eng., ASCE, Vol. (121), No. 11, pp. 773-781.

(Received June 10, 2013)